

Verification and application of beam-particle model for simulating progressive failure in particulate composites

Jibo Xing† and Liangqun Yu‡

Department of Civil Engineering, Yantai University, Yantai 264005, China

Jianjing Jiang‡†

Department of Civil Engineering, Tsinghua University, Beijing 100084, China

Abstract. Two physical experiments are performed to verify the effectiveness of beam-particle model for simulating the progressive failure of particulate composites such as sandstone and concrete. In the numerical model, the material is schematized at the meso-level as an assembly of discrete, interacting particles which are linked through a network of brittle breaking beams. The uniaxial compressive tests of cubic and parallelepipedal specimens made of carbon steel rod assembly which are glued together by a mixture are represented. The crack patterns and load-displacement response observed in the experiments are in good agreement with the numerical results. In the application respect of beam-particle model to the particulate composites, the influence of defects, particle arrangement and boundary conditions on crack propagation is approached, and the correlation existing between the cracking evolution and the level of loads imposed on the specimen is characterized by fractal dimensions.

Keywords: beam-particle model; particulate composites; progressive failure; meso-structure; fractal dimension.

1. Introduction

The simulating of progressive failure is important in understanding how the formation, evolution, and interaction of stress-induced microcracks lead to macrofracture. Particulate composites such as concrete and sandstone are heterogeneous or disordered materials which are very often considered as two-phase materials made of aggregates or grains and matrix. Density, porosity and mechanical properties are not identical at each point within a sample, which induces stress concentrations when subjected to mechanical loadings. The fracture process in particulate composites starts with microcracking. Microcracks are generally considered to develop from the weakest points and from the flaws or defects pre-existing among materials on various scales,

† Associate Professor

‡ Lecturer

‡† Professor

mostly due to debonding between matrix and aggregate (or grain). The generated microcracks grow together and form a localized crack which leads to the failure of the whole structure. Therefore, the micro- and meso-structure of the material should be taken into account for the modelling of progressive failure in particulate composites.

Most of the numerical models used for simulating progressive failure in particulate composites are macromechanical models and are based on the fictitious crack model proposed by Hillerborg *et al.* (1976). These models use the fracture energy as a material property and are suitable for structural calculations. But they have difficulties in correctly representing the failure mechanisms in heterogeneous materials. The main reason for this is that the material is assumed to be homogeneous, and heterogeneous meso-structure is not taken into consideration in these models. Although much empirical knowledge has been gathered, there are still numerous fundamental aspects that remain unsolved. Therefore, it is important to develop a numerical model to study what may really happen in particulate composites when taking into account their heterogeneous meso-structure in a somewhat realistic scale.

The most realistic scale used to simulate the fracture is certainly on the atomic level. Because of the existing limitations of computational capabilities, this idea is too ambitious to realize. However, with the development of fast computers, it has become possible to model the structure of the material at micro or meso level directly. The latest attempts are based on lattice techniques (Herrmann *et al.* 1989), which RILEM (The International Union of Testing and Research Laboratories for Materials and Structures) affirms in a report are a very promising tool in the study of microcracking of concrete under tension (Bascoul 1996). In the lattice model, the material is schematized as a network of beam elements in the zone of the specimen where cracks are expected. Different material properties are assigned to the respective beam elements in matrix, aggregates or grains and bonds. When the maximum tensile stress in a beam is larger than its strength, this beam is supposed to break and is removed from the mesh. It has been shown that crack patterns obtained with the model are in good agreement with the concrete fracture experimental observations. The main disadvantages of the model are that it is inapplicable for simulating compressive failure and the mass of the specimen under increasing compressive loadings would vanish using the model, because there is no compressive failure criterion available until now (Vervuurt *et al.* 1996). Furthermore, the lattice model can not cope with particle rotations and particle separations. Cracks induced under a compressive stress field are of the most interest because the particulate composites are under compressive stress most of the time in practice. As a result, the application scope of the lattice model is limited to some extent.

In order to resolve the weak points of the lattice model, a meso-mechanical beam-particle model solved using an iterative scheme has been proposed for simulating the progressive failure in the particulate composites (Wang and Xing 1990, 1991). Since the behaviour of the constituents was experimentally proved to be more brittle than particulate composite itself, the fracture of particulate composites may be studied by assuming the constituents of particulate composites to be linear elastic materials. The beam-particle model adheres to this assumption. In the model, the whole medium is divided into an assembly of discrete, interacting particle elements which are linked through a network of brittle breaking beam elements. The mechanical behaviour of particle elements is governed by the distinct element method (Cundall and Strack 1979) and finite element method. The propagation of the cracking process in particulate composites is mimicked by removing the beam element from the mesh as soon as the stress in the beam exceeds the strength assigned to that particular beam. The beam-particle model has the combined

advantages of both lattice model and distinct element model, not only suitable for simulating tensile, shearing and compressive fracture but also for simulating the postfailure behaviour, such as some fragments flying off with high velocity.

In the following sections, we will describe the fundamentals of the beam-particle model first, and then consider the most common situation where cracking takes place in the bulk of the material under compression as in the simulation examples. Numerical results obtained are compared with the experimental results. Moreover, the fractal geometry is utilized to evaluate the connectivity of cracking. The questions of what universal laws exist in the maximum load one has to apply to break the structure apart are also discussed in this paper. The main objective of the investigation is to demonstrate the validity of the model, but also attention is focused on simulating the way the cracks develop and finding final crack patterns.

2. Numerical model

In this paper, a beam-particle model is presented for simulating progressive failure in particulate composites. In the model, the material is schematized at the meso-level as a two dimensional assembly of particle elements and nearest-neighboring particles are connected through a lattice of elastic beam elements (Fig. 1). A real aggregate or grain in particulate composites may be composed of several particle elements. If a particle is created on one site where no aggregate or grain exists in reality, the particle is named a 'matrix particle' which functions as cementing material and transferring loadings. The rest of the particles which constitute an aggregate or grain are named 'reinforcing particles'. According to the types of two linked neighbouring particles, the beam elements can be classified into three types: 'reinforcing beam' which connects two reinforcing particles, 'matrix beam' which connects two matrix particles, and 'bond beam' which connects a reinforcing particle and a matrix particle. Different types of beam have different elastic and strength properties. The disorder or heterogeneity of particulate composites can be easily implemented in the numerical simulation of fracture process by varying the particle sizes and beam strength, etc. Voids and other defects pre-existing among materials can be modelled by breaking beam elements in advance.

The beam-particle model uses a step-by-step approach. Due to the fact that the material structure has been modelled in detail, the model becomes inherently more simple. Detailed descriptions of the model are as follows.

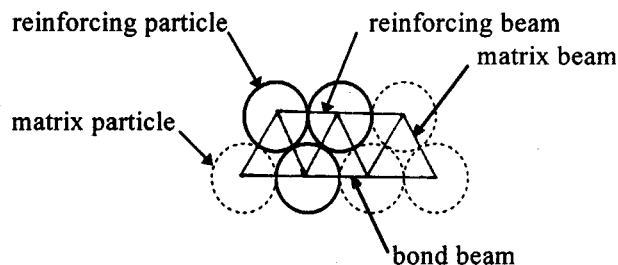


Fig. 1 Schematic representation of the beam-particle model

2.1. Force-displacement equations of beam element (Long et al. 1979)

For a beam element which links two nearest-neighboring particles, there are three continuous degrees of freedom on one node i (i.e., the center of a particle): the two coordinates x_i and y_i and one flexed beam angle θ_i . The beam is to be imagined having a certain thickness and can carry normal, shear and bending forces. One defines two relative displacement variables and three material dependent constants:

$$\Delta x = x_j - x_i, \quad \Delta y = y_j - y_i \quad (1)$$

$$s = EI/l, \quad \alpha = EA/l, \quad \beta = 14.4EI/(GA l^2) \quad (2)$$

where E =Young's modulus, G =shear modulus, A =area of the beam section, I =moment of inertia for flexion, l =spacing between two nodes of a beam. Then for a horizontal beam between nodes i and j , one has the longitudinal force:

$$N_{ij} = N_{ji} = \alpha \Delta x \quad (3)$$

the shear force:

$$Q_{ij} = Q_{ji} = \frac{6s}{(1+\beta)l} (\theta_i + \theta_j) - \frac{12s}{(1+\beta)l^2} \Delta y \quad (4)$$

and the flexural torques:

$$M_{ij} = \frac{(4+\beta)s}{1+\beta} \theta_i + \frac{(2-\beta)s}{1+\beta} \theta_j - \frac{6s}{(1+\beta)l} \Delta y \quad (5)$$

$$M_{ji} = \frac{(2-\beta)s}{1+\beta} \theta_i + \frac{(4+\beta)s}{1+\beta} \theta_j - \frac{6s}{(1+\beta)l} \Delta y \quad (6)$$

Similar formulas can be rewritten for vertical beams.

The fracture of the particulate composites takes place by removing in each load step the beam element as soon as its stress strength is exceeded. The stress strength σ_t is derived from the following equation:

$$\sigma_t = \eta N/A + \xi \text{Max}(|M_i, M_j|)/W \quad (7)$$

where N =normal or longitudinal force in the beam element, M_i and M_j =bending moments in node i and j of the beam element respectively, $A=d \times h$ =cross sectional area of the beam, d =beam thickness, $h=0.618l$ =height of the beam, $W=d \times h^2/6$, η =a scaling factor for the axial stress, ξ =a scaling factor for the bending force.

2.2. Motion laws of particle element

When beam elements are broken and removed, the particle elements freed can interact on each other based on the technique of distinct elements (Wang and Xing 1991). This technique simulates the discrete behavior of the medium by assuming that the motion of each particle may be modeled using Newtonian rigid-body mechanics with particular force-deformation and force-deformation rate contact laws. In general, the contact forces F_{cn} and F_{ct} in normal and tangential directions could be written as:

$$F_{cn} = F_{cn}(k_n, \delta_n, \delta_t) \quad (8)$$

$$F_{ct} = F_{ct}(k_t, \delta_n, \delta_t) \quad (9)$$

where δ_n and δ_t are the relative normal and tangential displacements between contacting particles i and j , and k_n and k_t are the normal and tangential stiffnesses.

Considering the i th particle and applying Newton's second law of motion yields:

$$\sum_{j=1}^N F_c^{ij} + F^i = m_i \ddot{x}_i \quad (10)$$

$$\sum_{j=1}^N M_c^{ij} + M^i = I_i \ddot{\theta}_i \quad (11)$$

where F_c^{ij} are the j contact forces on the i th particle, F^i represents the resultant non-contacting force on particle i , m_i is the particle mass, \ddot{x}_i is the linear acceleration of particle centroid, M_c^{ij} are the moments (about the particle centroid) resulting from contact forces F_c^{ij} , M^i is the resultant moment from non-contacting forces, I_i is the mass moment of inertia, and $\ddot{\theta}_i$ is the angular acceleration about the particle centroid.

When the linear and angular accelerations are resolved from Eqs. (10) and (11), the velocities and displacements can be obtained by integration over incremental timesteps using a central difference scheme, and then applying Eqs. (3) to (6) the forces in a beam can be determined from the new linear and angular displacements of particles connected by the beam during each timestep. The procedure is repeated until a satisfactory state of equilibrium or mode of failure results.

This distinct element model offers significant advantages for the analysis of multiple interacting, deformable and fractured bodies undergoing large displacements and rotations. In the model, the particle elements are capable of transmitting compressive loadings of post-failure, which makes up the deficiency of the lattice model. The main shortcoming of the distinct element model is that it cannot transmit tensile loadings. However the tensile loadings can be borne by the beam elements as mentioned above. Here it should be pointed out that in the beam-particle model the particles contain all the mass of beam-particle model and the beams do not carry any mass.

3. Experimental procedures and results

If the disorder or heterogeneity of the particulate composites is taken into account, the full similarity between the physical experiments and numerical simulations is too difficult to realize. As mentioned above, the main aim of the study is to test and verify the effectiveness of the beam-particle model. For convenience' sake, the particulate composites are supposed to be homogeneous in the following physical experiments and numerical simulation, i.e., the physical and mechanical properties of both reinforcing and matrix beams are all taken to be identical, even though the disorder or heterogeneity can be easily incorporated in the numerical simulation of fracture process by varying the particle sizes and beam strength, etc.

The physical experiments are conducted on specimens made of hexagonal close-packed rods of diameter 5.0 mm. The rod is carbon steel wire which has a mass density of $7.845 \times 10^3 \text{ kg/m}^3$. The rod assembly is glued together by a mixture whose mixing proportions of Portland cement 425[#] : epoxy resin (E-44) : ethylene diamine : dibutyl phthalate : toluene are 2 : 1 : 0.1 : 0.1 : 0.1 (by weight). The specimens are removed from their moulds one day after casting and are then cured

for three weeks in a laboratory condition (temperature 20°C, humidity 50%).

Two different shapes of specimens are tested, namely cube and rectangular parallelepiped. The dimensions of the cube and rectangular parallelepiped are $60 \times 60 \times 60$ mm and 60×150 mm with a thickness of 50mm respectively. Uniaxial compressive tests are performed in a hydraulic closed-loop testing machine, under a constant rate. The linear variable displacement transducers (LVDTs) and loadometer (BHR-4) for the axial displacement and load measurements are attached to the upper loading platen of the machine respectively. The IMP (i.e., isolated measurement pods) and IMPDAS (i.e., IMP data acquisition system) are applied to monitor and record the deformations and loads on the specimen.

The main experimental results for the compressive tests are presented in terms of crack pattern and load-displacement curve. The testing results on the cubic specimens are introduced first. Fig. 2 shows the vertical cross section of the specimen that has been loaded up to failure. It can be seen that the cracks are not continuous and on the whole the crack pattern appears as the well known hourglass failure mode. As a result of opening of cracks the volume of the material increases. The load-displacement response for the cubic specimen loaded up to 1.15 mm is shown in Fig. 3, from which it can be seen that the specimen tends to fail in a rather brittle manner.

Finally, Fig. 4 illustrates the case of the parallelepipedal specimen described above. From the crack pattern, it is apparent that the increase of the height to width ratio of the specimen improves the chances of finding a failure mode with one dominant shear crack. This has already been observed by Van Mier (1986).

4. Numerical results and discussion

The experiments described above have been analysed using the beam-particle model under the same test conditions. All of the simulations are done under uniform and vertical boundary displacement control. The time stepping scheme used an increment $\Delta t = 1\mu\text{sec}$ in the dynamic simulation. Table 1 gives the input parameters for numerical simulation, in which the mechanical properties of beam are determined from the macroscopic properties through inverse analyses.

4.1. Comparison with experimental results

The simulated progressive failure in both cubic and parallelepipedal specimens of particulate

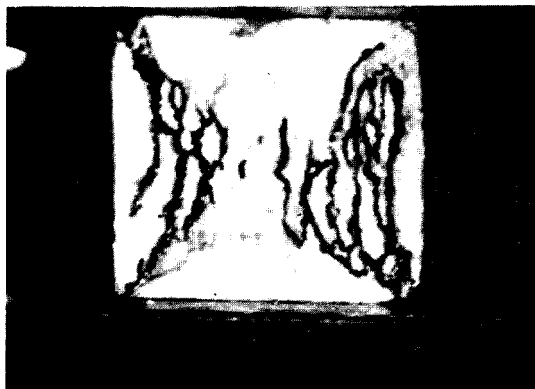


Fig. 2 Crack pattern of the cubic specimen loaded up to failure

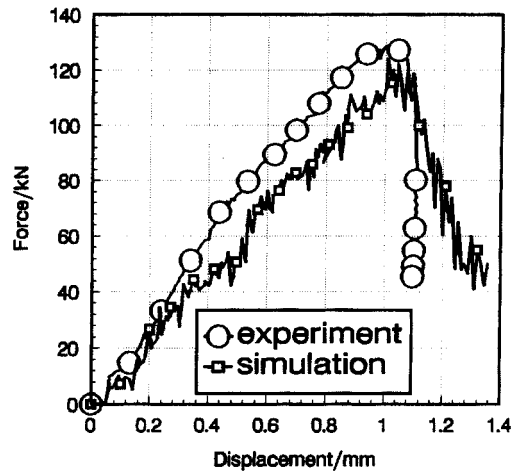


Fig. 3 Experimental and simulated load-displacement curves of the cubic specimen

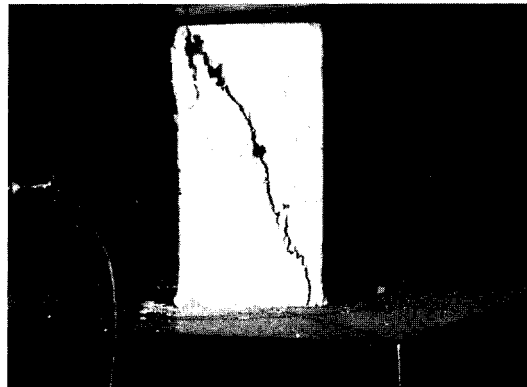


Fig. 4 Crack pattern of the parallelepipedal specimen loaded up to failure

composites are shown in Figs. 5 and 6. When the simulations are compared with the experiments as shown in Figs. 2 and 4, it can be noticed that large similarities exist in the respective crack patterns which have analogous shapes on the whole. As the height of the specimen is equal or close to its width, the well known hourglass failure mode is found, while for the specimen of larger height to width ratio, a failure mode with one dominant shear crack is predicted. In both modes, the cracks develop intermittently in the material, so many cracks and 'rock bridges' are formed. From the changes of pattern areas in both simulations or horizontal velocity vectors shown in Fig. 6, it can be obviously seen that the progressive dilation has occurred.

The load-displacement curve of the simulation with the beam-particle model on the cubic specimen is compared in Fig. 3. As seen from Fig. 3, the experimental curve is rather smooth, but the simulated curve evolves with snapback phenomenon. Although the post peak behaviour simulated is less brittle than the experimental outcome, the level and position of the peak load are approximately the same as observed by experiment.

Table 1 Input parameters for numerical simulation

Mechanical parameter	Value
Compressive strength of specimen	30 MPa
Young's modulus of beam	28 GPa
Shear modulus of beam	13 GPa
Compressive strength of beam	250 GPa
Tensile strength of beam	31 GPa
Normal and shear stiffness of particle	260 kN/mm
Friction angle	45°

4.2. Influence of defects and boundary conditions on crack propagation

In order to simulate the influence of the defects existing in the particulate composites, some voids are randomly generated in advance in the parallelepipedal specimen simulated just above, as shown in Fig. 7(a). Under the same loading conditions as in Fig. 6, the cracking process is shown in Fig. 7. In comparison with the results simulated in Fig. 6, the positions of the dominant shear cracks almost coincide, but the crack distribution in other parts are inconsistent owing to the influence of internal defects in the specimen.

In addition to defects, the influence of particle arrangement and boundary conditions on crack propagation is investigated next. The initial state of the simulated specimen is shown in Fig. 8(a). The loading conditions are all the same as used in Fig. 5 except that a small lateral boundary

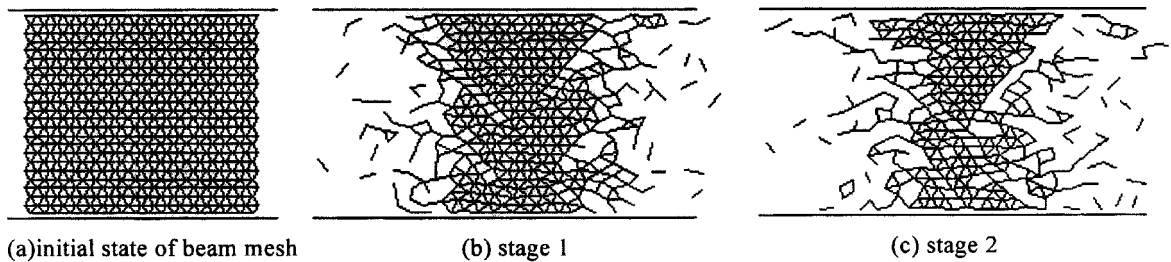


Fig. 5 Crack history of cubic specimen at different stages of loading

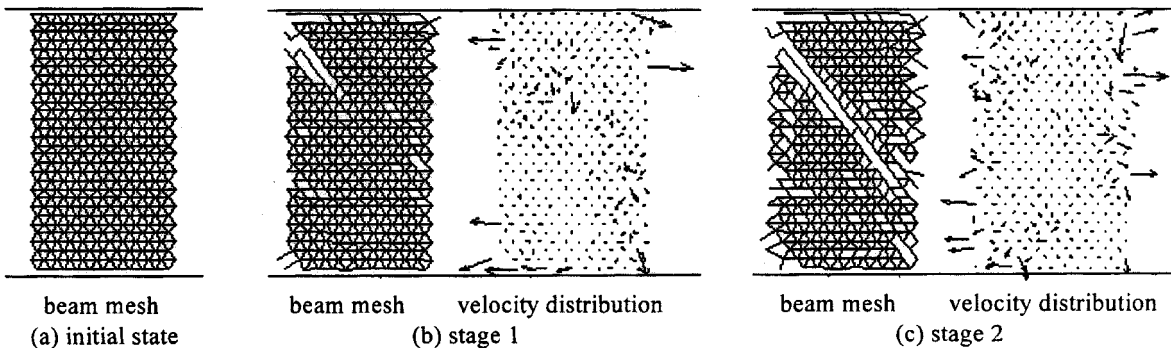


Fig. 6 Crack history of parallelepipedal specimen at different stages of loading

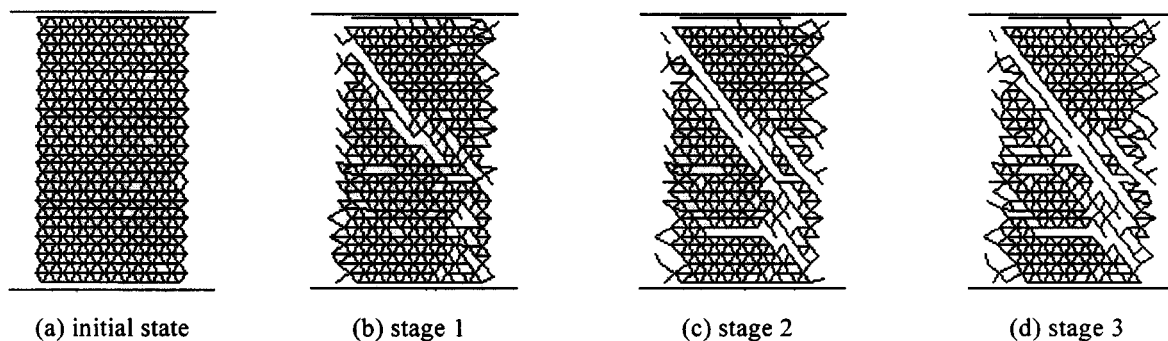


Fig. 7 Crack history of defective parallelepipedal specimen under compression

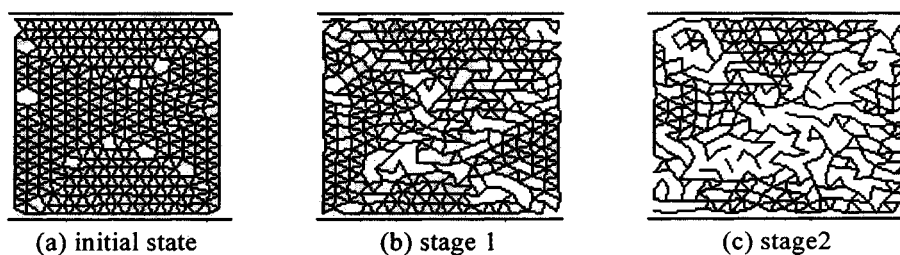


Fig. 8 Crack patterns with lateral boundary restraint

restraint is imposed upon the specimen. From the simulated results shown in Fig. 8, it may be seen that the failure mode is quite irregular and the cracking takes place around most of the voids.

4.3. Relation of fractal characteristics of cracking with the the load-bearing capacity

It is very important to discuss the correlation existing between the cracking evolution and the load-bearing capacity in the research on lifetime performance of materials (Bascoul 1996). In this paper, this question is approached using the theory of fractal geometry (Xie 1993). There are many methods to determine the fractal dimension of crack patterns, including the divider method, box-counting method and spectral method. Because the box-searching scheme (Cundall *et al.* 1979) is used to detect contacts between particles, it is quite convenient to apply the box-counting method to determine the fractal dimension of crack patterns without extra subdivision of problem space into boxes.

From an operative point of view, the box-counting method is implemented by generating a square grid of linear dimension ε_i and determining the number $N_i(E, \varepsilon_i)$ of boxes needed to cover the entire area E . The procedure is repeated with progressively smaller box sizes. Linear regression with the bilogarithmic data ($\log N_i$ versus $\log \varepsilon_i$) is performed, and the fractal dimension D is obtained from the slope of the best-fitting line.

A fractal dimension field [1.4, 1.6], which characterizes the relation between the cracking connectivity and the loading level, has been found through many repeats of numerical tests. As an example, Fig. 9 indicates the relationship between box size and number of boxes needed to cover the entire crack patterns of the cubic specimen under compression as shown in Fig. 5. Just before the load exceeds the compressive strength of the cubic specimen, the fractal dimension of the

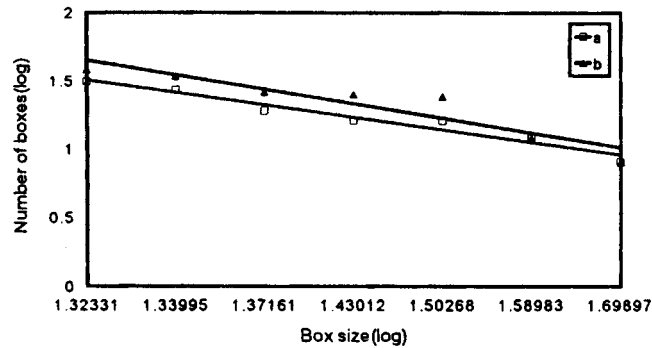


Fig. 9 Fractal dimension just before and after the compressive strength of the specimen is exceeded

crack patterns obtained from the slope of the best-fitting line *a* in Fig. 9 is 1.38, less than 1.4. When the load exceeds the compressive strength of the specimen and displacement equals 1.1 mm, the fractal dimension of crack patterns is increased to 1.71 (i.e., the slope of the best-fitting line *b*), much greater than 1.6. It should be conjectured that the fractal dimensions 1.4 and 1.6 would be regarded as the critical values to evaluate the connectivity of cracking and to describe load intensity. When the fractal dimension *D* of crack patterns is less than 1.4, the connectivity of cracking has not been well developed and the loading imposed on the specimen can be increased. When the fractal dimension *D* of crack patterns is greater than 1.6, the cracks have been fully intersected and the engineering performance of the specimen has become poor.

5. Conclusions

In this paper, an inherently simple beam-particle model is presented for simulating progressive failure of particulate composites such as concrete and sandstone. Two physical experiments have been done to verify the validity of the model. The crack patterns and load-displacement curve observed in the experiments are in good agreement with the numerical results. The numerical investigations show that several factors have influence upon the fracture behaviour of particulate composites. These factors include the defects, particle arrangement and boundary conditions. The main advantage of the model is that it can correctly capture the failure mode and the progressive dilation of a specimen under different loading conditions. In addition, with the theory of fractal geometry successfully implanted in the model, a correlation between the maximum compressive stress imposed on the specimen and the fractal dimension of crack patterns is found. Thus, the critical point just as the structure of a specimen totally collapses can be predicted according to the fractal dimension. Although the beam-particle model is still relatively crude at the moment, it is firmly believed that through further improving work the model will become a more useful tool for simulating progressive failure and explaining the failure mechanisms of particulate composites.

Acknowledgements

The authors are grateful for the financial support of the National Natural Science Foundation of

China and the Natural Science Foundation of Shandong Province. They also owe many thanks to Professor Yongjia Wang for beneficial discussions.

References

- Bascul, A. (1996), "State of the art report, Part 2: Mechanical micro-cracking of concrete", *Materials and Structures*, **29**, 67-78.
- Cundall, P.A. and Strack, O.D.L. (1979), "A discrete numerical model for granular assemblies", *Geotechnique*, **2**(1), 47-65.
- Herrmann, H.J., Hansen, H. and Roux, S. (1989), "Fracture of disordered, elastic lattices in two dimensions", *Phys. Rev.*, **B39**(1), 637-648.
- Hillerborg, A., Modeer, M. and Petersson, P.E. (1976), "Analysis of crack formation and crack growth in concrete by means of fracture mechanics and finite elements", *Cement and Concrete Research*, **6**(6), 773-782.
- Long, Y.Q. and Bao, S.H. (1979), *Structural Mechanics – Part 2*, Beijing, Higher Education Press, 298-303.
- Van Mier, J.G.M. (1986), "Multiaxial strain softening of concrete", *Materials and Structures*, **19**, 179-200.
- Vervuurt, A., Schlangen, E. and Van Mier, J.G.M. (1996), "Tensile cracking in concrete and sandstone, Part 1: Basic instruments", *Materials and Structures*, **29**, 9-18.
- Wang, Y.J. and Xing, J.B. (1990), "The improvement of distinct element method and its application in engineering", *Application of Numerical Methods in Geotechnical Engineering*, Shanghai, Tongji University Press, 245-250.
- Wang, Y.J. and Xing, J.B. (1991), *Distinct Element Method and its Applications in Soil and Rock Mechanics*, Shenyang, Northeastern University Press, 60-89.
- Xie, H. (1993), *Fractals in Rock Mechanics*, Geomech. Research Ser. Balkema, Rotterdam/Brookfield, 58.